

Biomechanical Effects of Stiffness in Parallel With the Knee Joint During Walking

Kamran Shamaei*, *Student Member, IEEE*, Massimo Cenciari, *Member, IEEE*, Albert A. Adams, Karen N. Gregorczyk, Jeffrey M. Schiffman, and Aaron M. Dollar, *Senior Member, IEEE*

Abstract—The human knee behaves similarly to a linear torsional spring during the stance phase of walking with a stiffness referred to as the knee quasi-stiffness. The spring-like behavior of the knee joint led us to hypothesize that we might partially replace the knee joint contribution during stance by utilizing an external spring acting in parallel with the knee joint. We investigated the validity of this hypothesis using a pair of experimental robotic knee exoskeletons that provided an external stiffness in parallel with the knee joints in the stance phase. We conducted a series of experiments involving walking with the exoskeletons with four levels of stiffness, including 0%, 33%, 66%, and 100% of the estimated human knee quasi-stiffness, and a pair of joint-less replicas. The results indicated that the ankle and hip joints tend to retain relatively invariant moment and angle patterns under the effects of the exoskeleton mass, articulation, and stiffness. The results also showed that the knee joint responds in a way such that the moment and quasi-stiffness of the knee complex (knee joint and exoskeleton) remains mostly invariant. A careful analysis of the knee moment profile indicated that the knee moment could fully adapt to the assistive moment; whereas, the knee quasi-stiffness fully adapts to values of the assistive stiffness only up to ~80%. Above this value, we found biarticular consequences emerge at the hip joint.

Index Terms—Human walking, knee biomechanics, lower extremity exoskeleton, parallel stiffness, quasi-passive mechanism, variable stiffness.

I. INTRODUCTION

UNDERSTANDING how human locomotion and the biomechanics of lower extremity joints are altered during interaction with external engineered systems and changes in the environment is of importance to several fields, including orthotics and prosthetics [1]–[6], rehabilitation and physical therapy [7]–[9], and fundamental physiology and biomechanics [10]–[12]. Locomotor adaptation in the lower extremity joints is typically studied by exposing the human (or relevant species) lower limbs to externally applied mechanical impedances and perturbations [13], externally added mass [14], [15], or to uneven terrains in locomotion tasks [16], [17]. A common message

Manuscript received September 13, 2014; revised December 16, 2014 and April 20, 2015; accepted April 28, 2015. Date of publication April 30, 2015; date of current version September 16, 2015. Asterisk indicates corresponding author.

*K. Shamaei is with the Department of Mechanical Engineering and Materials Science, Yale University, New Haven, CT 06511 USA (e-mail: kamran.shamaei@yale.edu).

M. Cenciari is with the Neurologische Universitätsklinik Freiburg Breisacher.

A. A. Adams and K. N. Gregorczyk are with the US Army Natick Soldier Research, Development and Engineering Center.

J. M. Schiffman is with the Liberty Mutual Research Institute for Safety.

A. M. Dollar is with Yale University.

Color versions of one or more of the figures in this paper are available online at <http://ieeexplore.ieee.org>.

Digital Object Identifier 10.1109/TBME.2015.2428636

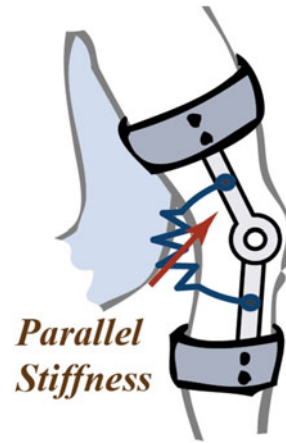


Fig. 1. Knee complex is defined as the combination of the knee joint and exoskeleton. This study investigates the interaction between human knee joint and parallel stiffnesses externally applied by an exoskeleton.

from these research undertakings is that the human body can adapt to external environmental changes to exhibit stable gait.

Compliance at the leg and joint level plays an essential role in achieving stable gait and is implemented through stiffness and quasi-stiffness modulation in lower extremities [18]–[22]. Dynamic and static stiffness of the lower extremity joints have been characterized by researchers using external perturbation in conjunction with statistical system-identification techniques [13], [23], [24], static loading tests [25], and *in vitro/in vivo* validation of muscle models and electromyography [26]–[28]. Researchers have also explored lower extremity function in response to series stiffnesses and found that upon a change in the surface stiffness, lower extremities adapt such that the overall stiffness at the center of mass remains invariant [29], [30]. It is unclear at this point, how the human body responds to external mechanical impedances implemented in parallel.

Recently, there has been a growing interest in studying the behavior of lower extremity joints in interaction with parallel assistive systems. These studies could prove beneficial for the development of exoskeletons meant for gait assistance with able-bodied users [3], [31]–[36], rehabilitation orthoses meant for physical therapy [37], [38], and assistive orthoses meant for gait assistance to impaired users [39]–[41]. To this end, researchers have exploited the potentials of robotic exoskeletons to study human motor response to parallel perturbations/assistance to the ankle [1], [3], [34], [42], knee [31], [32], and hip joint [35], [38], [43].

In this study, we explore the interaction of the knee joint with externally applied parallel stiffnesses using a pair of quasi-passive robotic knee exoskeletons. The knee joint demonstrates

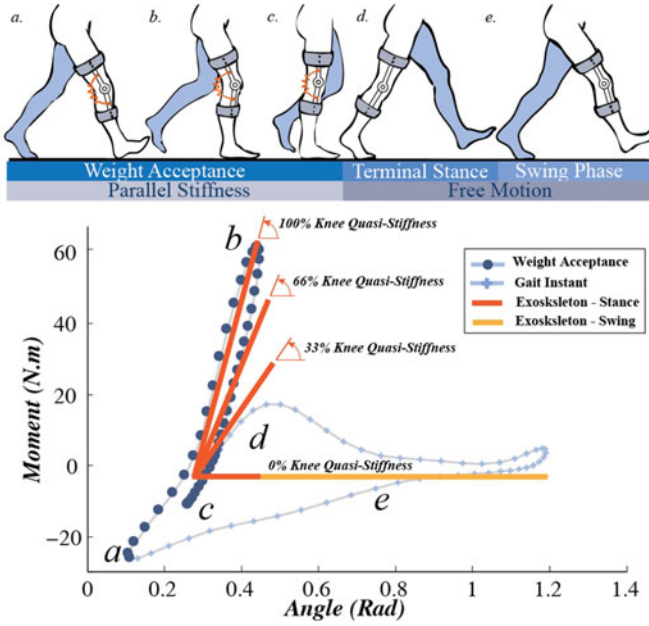


Fig. 2. Top: The exoskeleton implements a high-stiffness spring in the weight acceptance phase of the gait and a low-stiffness spring (with negligible stiffness) throughout the rest of the gait cycle. Bottom: The exoskeleton implements four levels of spring stiffness including 0%, 33%, 66%, and 100% of the estimated knee quasi-stiffness.

several major functions in walking—it primarily supports the weight of the body, absorbs the shock resulting from heel strike, and flexes in the swing phase to increase foot clearance and obstacle avoidance, allowing the leg to move forward and initiate the next gait cycle [45]. Each exoskeleton implements a spring in parallel with the knee joint during the stance phase and allows free motion throughout the rest of the gait cycle. This concept is schematically shown in Fig. 1. We chose to study the knee joint because it demonstrates a simple spring-like behavior during the stance phase of gait, which enables us to simply implement a spring in parallel to investigate the knee interaction with external stiffnesses [22], [44].

The human knee joint experiences three consecutive phases in a gait cycle: 1) substantial loading in the weight acceptance phase (first ~40%, as depicted in Fig. 2 points *a* to *c*), 2) moderate loading in the terminal stance (~40%–63%, as shown in Fig. 2 points *c* to *d*), and 3) a swing phase (points *d* to *e* in Fig. 2) [22], [44]–[48]. It demonstrates a linear flexion stage (points *a* to *b* in Fig. 2), and a linear extension stage (points *b* to *c* in Fig. 2) in the weight acceptance phase of gait [22], [44].

The quasi-stiffness is defined as the coefficient of a first-order polynomial regressed to the moment-angle data of a lower extremity joint during a period of gait. Quasi-stiffness is used to provide a simplified understanding of the overall behavior of the lower extremity joints in the linear loading phases of gait [20], [49]–[54]. Previous research showed that the knee quasi-stiffness in the flexion and extension stages of the weight acceptance phase tended to be identical at the preferred gait speed implying that the knee behaves close to a linear torsional spring at the preferred gait speed [22], [44]. Accordingly, we model the moment-angle behavior of the knee joint during the

TABLE I
DEFINITION OF PARAMETERS IN WEIGHT ACCEPTANCE PHASE

Parameter	Definition	Normalized
Knee Joint	Anatomical knee joint	
Knee Complex	Combination of knee joint and exoskeleton (if the condition includes the exoskeleton)	
K_K (Nm/kg · rad)	Knee joint quasi-stiffness	K_K
K_C (Nm/kg · rad)	Knee complex quasi-stiffness	K_C
K_E (Nm/kg · rad)	Exoskeleton stiffness	K_E
K_P (Nm/kg · rad)	Parallel stiffness (K_E and K_S in series)	K_P
M_K (Nm/kg · rad)	Knee joint loading effort	M_K
M_C (Nm/kg · rad)	Knee complex loading effort	M_C
M_E (Nm/kg · rad)	Exoskeleton parallel assistive	M_E
M_P (Nm/kg · rad)	Parallel assistive (equal to M_E)	M_P
K_S (Nm/kg · rad)	Interface series stiffness	–
θ_K (rad)	Knee joint excursion	–
θ_C (rad)	Knee complex excursion	–
θ_E (rad)	Exoskeleton excursion	–
θ_S (rad)	Interface series excursion	–

weight acceptance phase at the preferred gait speed by a linear torsional spring with a stiffness equal to the knee quasi-stiffness (K_K). Table I lists the definition of all the parameters used throughout this paper.

This paper focuses on investigating the interaction between the human knee joint (characterized by a quasi-stiffness K_K) and a spring (with stiffness K_P) implemented in parallel with the knee joint only during the weight acceptance phase. To this end, several hypotheses were formulated and tested as follows.

- 1) It was hypothesized that the overall behavior of the knee complex, which is the combination of the knee joint and the exoskeleton, would remain linear. Therefore, the knee complex behavior is expressed by the following two equations:

$$K_C = K_K + K_P \quad (1)$$

and

$$M_C = M_K + M_P. \quad (2)$$

In these equations, K_C is the knee complex quasi-stiffness. The moment of the knee complex (M_C) is expressed as the summation of the knee joint moment (M_K) and parallel moment (M_P).

- 2) It was also hypothesized that the knee joint quasi-stiffness and moment in the weight acceptance phase would change in response to the presence of the parallel exoskeletal stiffness and moment such that the overall quasi-stiffness and moment of the knee complex would remain invariant in response to parallel stiffnesses.

In other words, an increase in K_P in (1) is negated by a corresponding decrease in K_K such that the overall knee complex quasi-stiffness remains constant, namely

$$\Delta K_C = 0, \quad \text{therefore } \Delta K_K = -\Delta K_P \quad (3)$$

and similarly

$$\Delta M_C = 0, \quad \text{therefore } \Delta M_K = -\Delta M_P. \quad (4)$$

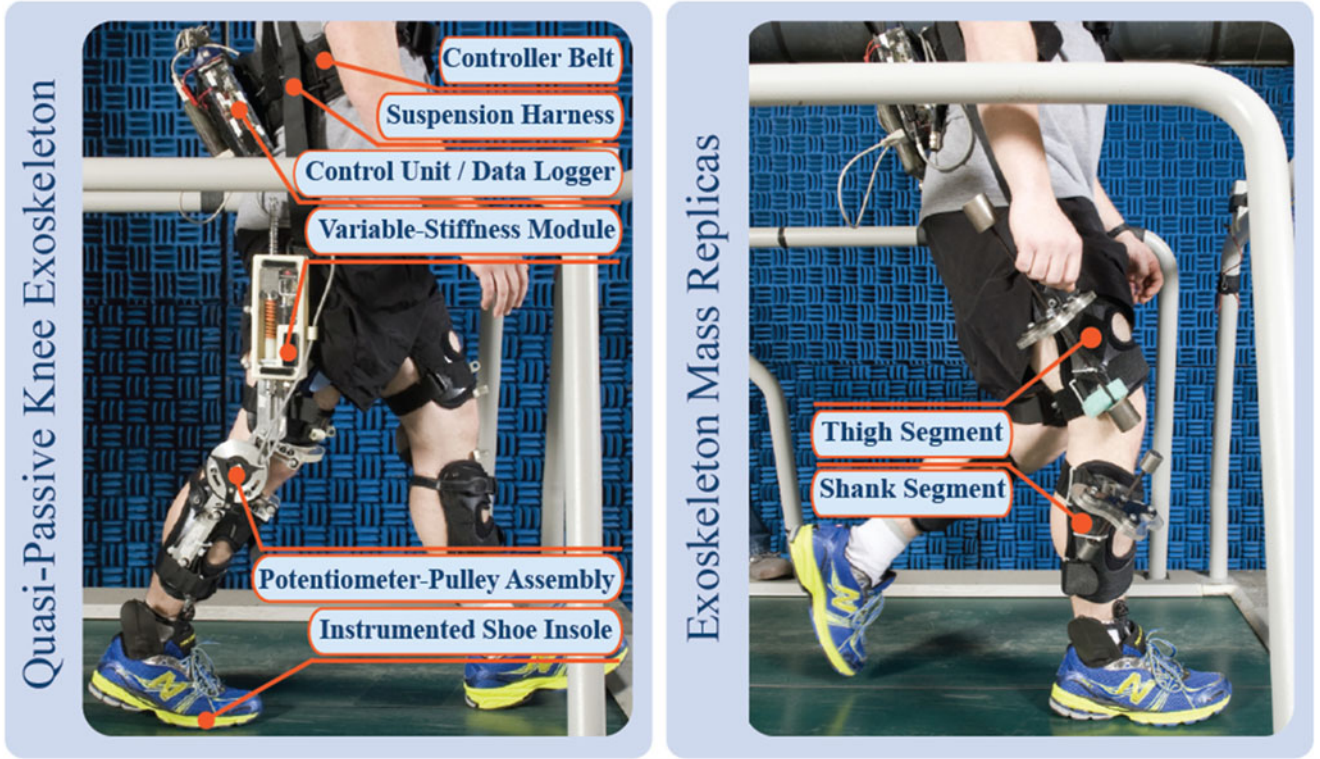


Fig. 3. Left: A volunteer walking with the quasi-passive knee exoskeleton. The control unit is mounted on a belt, and wirelessly transfers the data to a host computer. The exoskeleton and the controller are suspended with a harness from the shoulder. The exoskeleton is composed of a variable-stiffness module mounted on an adjustable knee brace equipped with a potentiometer-pulley assembly. Right: A joint-less replica device that has a mass distribution similar to that of the exoskeleton.

- 3) Finally, it was hypothesized that the mass and articulation of an exoskeleton could affect the kinematic and kinetic patterns of the knee joint.

To test these hypotheses, we used the quasi-passive exoskeletons in a series of experiments [see Fig. 3 (left)]. When using the knee exoskeleton, four levels of external stiffness were implemented in parallel with the knee joint, but only during the stance phase. Furthermore, the effects of the mass and articulation of the exoskeleton on the mechanical performance of the lower extremity joints (especially the knee joint) were studied using a pair of joint-less replicas of the exoskeleton with a mass distribution that was similar to those of the exoskeletons [see Fig. 3 (right)].

II. MATERIALS AND METHODS

A. Exoskeletal Devices

1) *Quasi-Passive Knee Exoskeleton*: When worn on a user, the quasi-passive knee exoskeleton implements a spring in parallel with the knee joint in the weight acceptance phase of gait and allows free motion during the terminal stance and the swing phases, as shown in Fig. 3 (left) and detailed in [39]. The exoskeleton mechanism includes two springs: a compliant spring (with negligible stiffness $K_L \sim 0$; see Fig. 4) that remains engaged throughout the gait cycle and an interchangeable high-stiffness spring (with stiffness K_H) that is engaged only in the weight acceptance phase of the gait cycle as schematically

shown in Fig. 2 (top). The primary function of the compliant spring is to return the exoskeleton shaft to the original reset position without applying considerable moment to the knee. The overall mechanical behavior of this system is shown in Fig. 4 (left), where the moment-angle graph of the exoskeleton is plotted over a typical moment-angle graph of human knee. The engagement mechanism is detailed in our previously published work [39].

The exoskeleton determines the engagement/disengagement of the high-stiffness spring according to the status of an instrumented foot insole that has toe and heel force sensors, and the angular knee joint velocity obtained as the readout derivative (defined as the difference between the current and previous angle) of a potentiometer incorporated in the exoskeleton joint. The high-stiffness spring is engaged at the beginning of the weight acceptance phase and disengaged when the foot is flat (both the heel and toe are on the ground), which in combination with the mechanism mechanical latency, roughly coincides with the end of the weight acceptance phase of the gait cycle. Table III includes the average time at which the exoskeleton spring was disengaged. It is worth noting that the spring was engaged exactly at the beginning of the gait cycle, considering that the mechanism engagement was initiated in the extension period of the swing phase [39].

2) *Moment-Angle Characterization of the Exoskeleton*: Fig. 4 (right) schematically illustrates the configuration of the exoskeleton springs and latching mechanism, which suggests

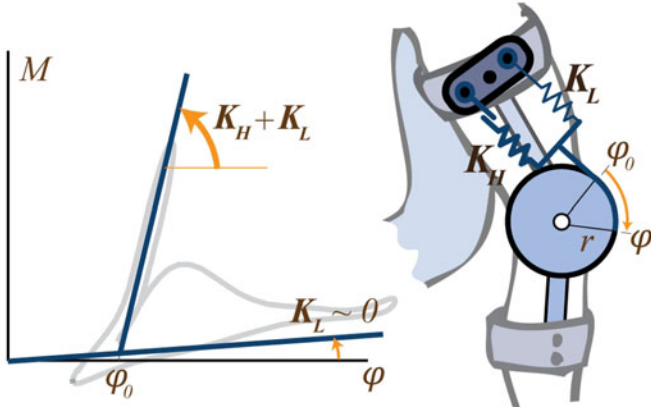


Fig. 4. Left: The moment-angle characterization of the exoskeleton. K_H is the constant of the high-stiffness spring, K_L is the constant of the low-stiffness spring, ϕ_0 is the angle of engagement, M is the exoskeleton moment, and φ is the exoskeleton angle. Right: Schematic model of the exoskeleton. A clutch mechanism engages/disengages the high-stiffness spring, whereas the low-stiffness springs (with negligible stiffness) remains engaged throughout the gait cycle.

the following equation for the exoskeleton stiffness:

$$K_E = \begin{cases} (K_L + K_H) \cdot r^2 & \text{engaged} \\ K_L \cdot r^2 & \text{disengaged} \end{cases} \quad (5)$$

and the following equation for the exoskeleton moment [39]:

$$M_E = \begin{cases} K_L \cdot r^2 \cdot \varphi + K_H \cdot r^2 \cdot (\varphi - \phi_0) & \text{engaged} \\ K_L \cdot r^2 \cdot \varphi & \text{disengaged.} \end{cases} \quad (6)$$

Here, $r = 5$ cm is the exoskeleton pulley radius, $K_L = 5$ N · m/rad is the constant of low-stiffness spring, φ is the knee angle, and ϕ_0 is the angle at which the high-stiffness spring is engaged. The values of φ and ϕ_0 and the engagement status of the high-stiffness spring for both left and right exoskeletons are continuously transferred to a host computer through the wireless communication module of the exoskeletons.

One of the questions that the current study intends to address is how the spring-type behavior of the human knee changes when an externally applied *parallel* stiffness is assisting during the stance phase. It is important to note that to ideally study this problem, the exoskeletal spring should be rigidly implemented between the femur and the tibia in the weight acceptance phase of gait, which is highly challenging. In reality, the exoskeleton spring interacts with the human leg through a series of compliant interfaces including the soft biological tissues of the leg and the cuffs and attachments of the exoskeletal devices, which are not completely rigid. These compliant interfaces can lead to an effective parallel stiffness that is different from the desired knee quasi-stiffness. Therefore, to account for the possible effects, the behavior of the interface was approximated by an additional series spring (with stiffness K_S) between the exoskeleton spring and the leg, as schematically shown in Fig. 5, and the overall parallel stiffness perceived by the anatomical knee joint can be estimated as

$$K_P = \frac{K_E K_S}{K_S + K_E}. \quad (7)$$

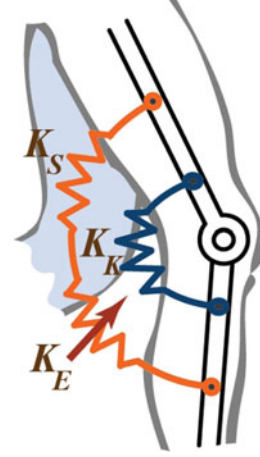


Fig. 5. Schematic model of the knee complex comprising the knee equivalent spring (K_K), exoskeleton spring (K_E), and a spring that models the interface materials (K_S) including the biological soft tissues of the leg and exoskeleton compliant components. The assistance conditions included modulation of K_E , whereas the intention of this study was to investigate the effect of parallel spring on the spring-type behavior of the knee joint.

3) *Exoskeleton Mass Replica*: To investigate the effects of the exoskeleton mass and inertia on the biomechanics of the knee, we fabricated a joint-less replica of the exoskeleton for each leg termed mass replicas. As shown in Fig. 3 (right), the mass replicas are composed of thigh and shank embodiments that comprise five identical steel cylinders assembled on a pair of thigh and shank cuffs similar to those of the exoskeleton. The mass, center of mass, and moment of inertia of the mass replicas and exoskeletons are nearly identical. The mechanical properties of the thigh and shank segments of the exoskeleton were estimated in SolidWorks (Dassault Systèmes SolidWorks Corp., Waltham, MA, USA) as reported in Table II.

B. Subjects

Nine healthy adult volunteers were recruited from US Army Soldiers assigned to Headquarters, Research, and Development Detachment of Natick Soldier System Center. Inclusion criteria were a body height between 1.50 and 1.90 m and a body weight less than 130 kg according to the size limitations of the fabricated exoskeletons. Table III lists the demographics of the volunteers, including the means and standard deviations (SD) of mass, height, and age of each volunteer. Written informed consent was obtained from each volunteer enrolled in this study prior to participation. This study protocol was approved by the Yale University Institutional Review Board, Human Use Review Committee of United States Army Research Institute of Environmental Medicine, Army Human Research Protections Office, and Battelle Institutional Review Board in accordance with DoD 3216.02, protection of human subjects. The experimental conditions included walking on a custom-made force plate treadmill (AMTI, Watertown, MA, USA). The treadmill comprises two synchronized treadmill belts positioned side by side, each on a separate force platform with a gap smaller than 1 cm. We used a ten-camera motion capture system (Qualysis,

Gothenberg, Sweden) and Qualisys Track Manager Software to track lower limb markers and calculate kinematic profiles at 1000-Hz frequency.

C. Experimental Conditions

The hypotheses were tested experimentally across the following six experimental conditions of treadmill walking.

- 1) Control Condition (CTRL): Without wearing the exoskeletons or mass replicas.
- 2) Exoskeleton Mass (MASS): Wearing the joint-less mass replicas.
- 3) Exoskeleton Articulation (0%): Wearing the exoskeleton unpowered with exoskeleton steel tendon detached.
- 4) –6) Exoskeleton Stiffness (33%, 66%, and 100%): Wearing the exoskeleton with assistance spring stiffnesses equivalent to 33%, 66%, and 100% of the quasi-stiffness of the anatomical knee estimated during normal walking at preferred gait speed.

To size the exoskeleton spring (K_E), we used a previously developed statistical model to estimate anatomical knee quasi-stiffness (K_K) in the weight acceptance phase of gait based on the subject's body size as [22]

$$K_K = 5.21W\sqrt{H^3} - 7.50W\sqrt{H} - 5.83WH + 11.64W - 6 \quad (8)$$

where W (kg) is the mass and H (m) is the height of the volunteer. This model has shown a 9% error of estimation and was established on data from volunteers with a wide range of masses (from 67.7 to 94.0 kg) and heights (from 1.43 to 1.86 m) [22]. Once the volunteer's K_K was estimated using (8), this value was used for condition 6 and it was then scaled to 33% and 66% for conditions 4 and 5, respectively. The values of gait speed, the estimated subject's quasi-stiffness, and the spring constants of the high-stiffness springs used for each volunteer are reported in Table III.

D. Experimental Protocol

The study volunteers had three visits in total, including two orientation sessions and one data collection session. On all visits, the participants wore shorts, t-shirts, socks, and their own athletic shoes. The three visits took place within a single week with one to two day(s) in between to provide rest and prevent any fatigue that could affect the results. Volunteers' mass and height were measured on the first visit to estimate each volunteer's K_K using (8), and size the K_E for the assistance conditions as described in the in the previous paragraph and reported in Table III.

1) *Orientation Sessions*: Two orientation sessions were included prior to the data collection session to allow the volunteers to become familiar with walking, while wearing the exoskeletons. On the first visit, participants walked on the treadmill for 3 min at 4.83 km/h to become familiar with treadmill walking, after which they were given a 3–5-min rest break. Each participant was then instructed to walk on the treadmill with a speed that slowly increased from the zero-speed state up to a self-selected comfortable pace. This pace was then used as the preferred gait speed throughout the experiments. Next, the

TABLE II
MASS PROPERTIES OF THE EXOSKELETON

Side	Segment	Weight (kg)	I_{xx} (kg · m ²)	I_{yy} (kg · m ²)	I_{zz} (kg · m ²)
Right	Thigh	1.68	0.02370	0.02312	0.00211
	Shank	0.77	0.00217	0.00249	0.00122
Left	Thigh	1.81	0.02370	0.02312	0.00211
	Shank	0.82	0.00217	0.00249	0.00122

exoskeleton was fitted on the volunteers, while seated, and the alignment of the exoskeleton joint with the knee joint was ensured. In an effort to minimize the vertical migration of the exoskeleton, suspension harness straps were also put on the volunteer and fastened to the controller belt, which was strapped around the chest and shoulders. Finally, the tension of the suspension straps was adjusted as the volunteers slowly stood up. The volunteers were asked to walk overground wearing the exoskeletons and mass replicas for each of the experimental conditions with the exception of the control condition. For each condition, the subjects walked overground for about 640 m at their own pace, covering a distance approximately equivalent to the distance covered in 8 min of treadmill walking. A 5-min seated rest break was given to the volunteers before they walked on the treadmill in the same condition for 8 min at their preferred gait speed. The order of the conditions for the first session was ordered from condition 2 to condition 6, and not randomized across volunteers.

The second orientation session included only treadmill walking trials of 10-min duration. The order of the six conditions was randomized (using a 6×6 Latin squares design) for each volunteer. The order of the conditions during each volunteer's second orientation session was the same as the order followed during the volunteer's data collection session (third and last session). To summarize, volunteers walked a total of 18 min on the treadmill and about 10 min overground for each experimental condition during the first two orientation sessions to become more familiar with walking while wearing the exoskeletal device.

2) *Data Collection Sessions*: Reflective markers were placed on body landmarks according to the convention described in [55], with slight differences in that four-marker clusters were placed on the shank and the thigh such that the exoskeleton cuffs could fit on the limbs without blocking their visibility from the ten cameras. Additionally, a four-marker cluster was placed on the chest to track the trunk and pelvis as a single segment. Within each trial, a 30-s long data recording was taken after 4 min from the start of the trial. Additional details can be found elsewhere [56].

E. Kinematic and Kinetic Analysis

Visual3D software (C-Motion, Gaithersburg, MD, USA) was used to calculate the lower extremity joint angles and moment profiles for all conditions. First, the moment of inertia of the shank, thigh, and trunk segments of the models in Visual3D were updated by including those of the exoskeleton and mass replicas listed in Table II. These adjusted values included the

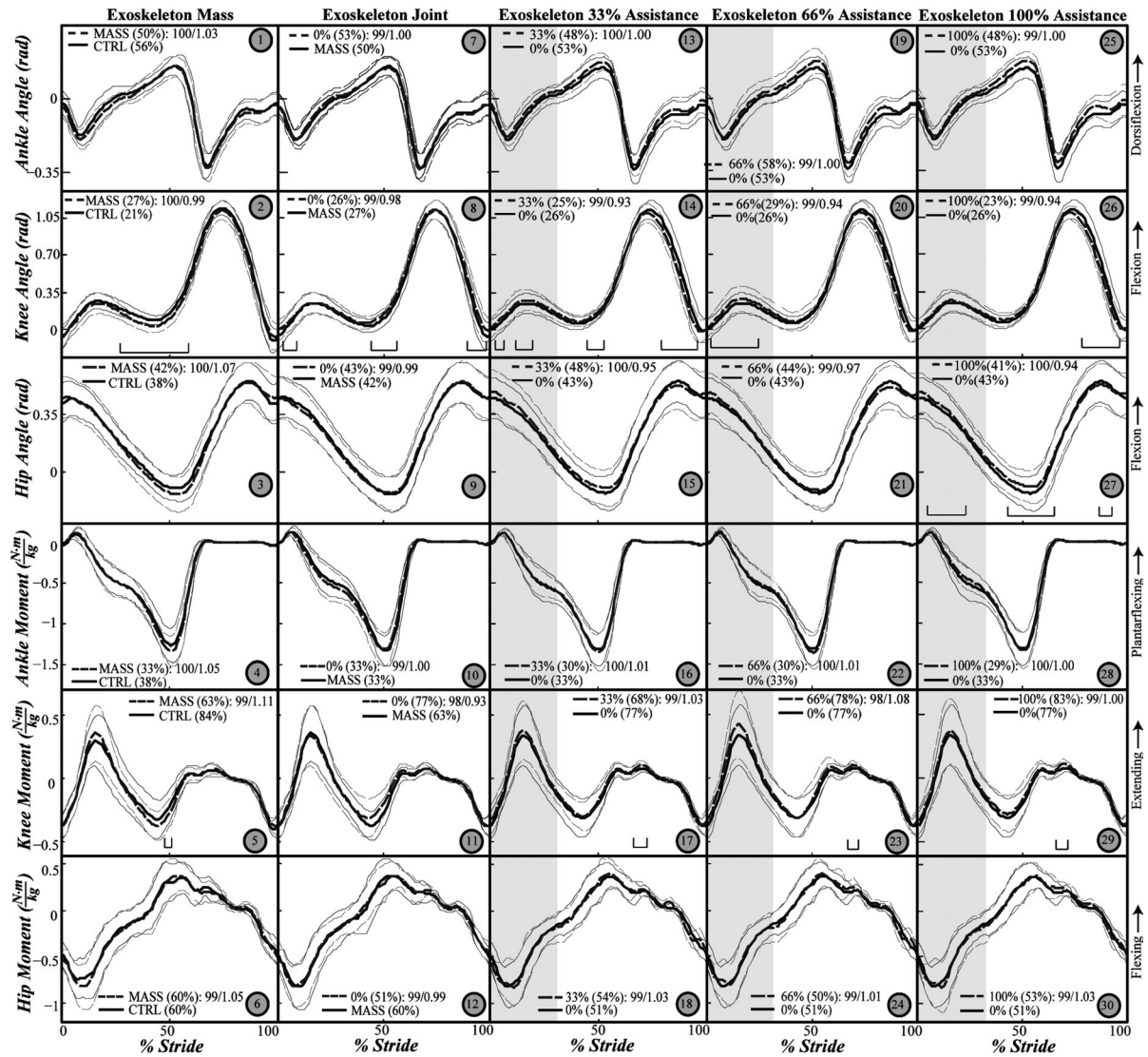


Fig. 6. Intersubject mean angle profiles on top half and moment profiles on bottom half as indicated on the left side of the image. The title of each column refers to the condition of interest (dashed trace) and the profile of the reference condition is shown with a solid trace. CTRL stands for normal walking (no exoskeleton), MASS stands for the mass replica condition (no articulation), and 0% till 100% stand for walking conditions wearing the exoskeletal devices with level of assistance indicated as % of the estimated human knee quasi-stiffness. The comparison is made between MASS and CTRL, 0% and MASS, 33% and 0%, 66% and 0%, and 100% and 0%. The thick lines indicate the intersubject mean profiles, and the thin lines boundaries are the ± 1 SD around the mean. Within each box and for each trace, the CV is reported between parentheses R^2 /scale of the regression comparison is also indicated for the comparison trace. The value of R^2 indicates how similar the profile patterns are, and the value of scale indicates how much the profiles are scaled. The values of R^2 /scale for the MASS condition are presented with respect to CTRL condition, the 0% condition with respect to the MASS condition, whereas the 33%, 66%, and 100% assistance conditions are presented with respect to 0%. On the bottom of each graph box, horizontal brackets are plotted to indicate the periods during which the two profiles are significantly different from each other.

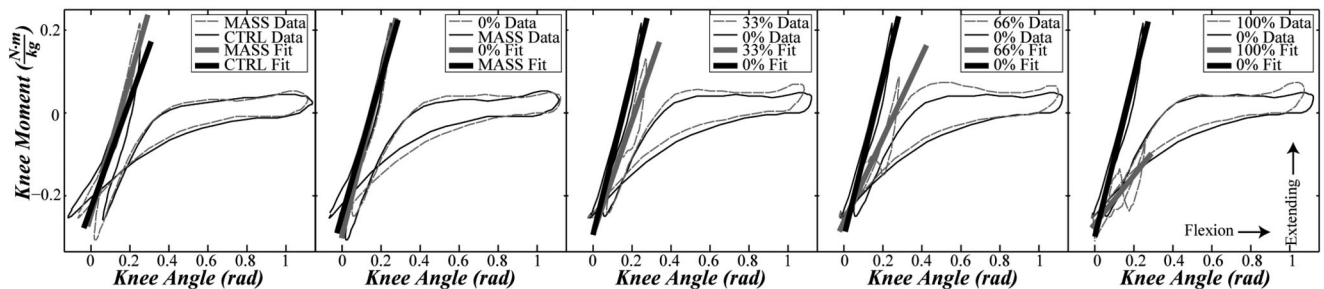


Fig. 7. Intersubject mean moment-angle graphs of the knee joint. The boxes include the graphs of CTRL and MASS, MASS and 0%, 0% and 33%, 0% and 66%, and 0% and 100%. The graphs also include linear fits to the moment-angle graphs of the weight acceptance phase.

human limbs and exoskeleton components. Inverse dynamics analysis was then performed to obtain the moment profiles of the ankle and hip joints and knee complex in the sagittal plane for the left and right side. The kinetic and kinematic intrasubject profiles of the left side and right side were averaged to obtain the final mean profiles. A third-order Butterworth filter with cutoff frequency of 8 Hz was used to filter the kinetic and kinematic profiles. The rest of the analyses were carried out in MATLAB (Mathworks, Natick, MA, USA). The exoskeleton moment was calculated using (6) and the angular data received from the exoskeleton. To approximate the moment of the knee joint in the sagittal plane, the synchronized moment of the exoskeleton was subtracted from the moment of the knee complex assuming that the axis of exoskeleton joint and knee joint were aligned.

F. Profiles Comparison Measures

The gait cycles were identified by the right heel strikes. Four consecutive gait cycles for each trial were identified from the force plate signals and complete marker data. We also verified that the calculated intrasubject averages for the joint angle and moment profiles from the four consecutive cycles were consistent among all trials. Additionally, the intrasubject mean profiles of the joint angles were normalized with respect to the standing configuration and the moment profiles with respect to the body mass [57]. The intersubject mean and SD of angle and moment profiles were subsequently obtained from the corresponding intrasubject mean profiles. The intersubject mean moment and angle profiles in the sagittal plane are plotted in Fig. 6. The coefficient of variability (CV; described elsewhere [47]) was calculated for each profile using the mean and SD profiles.

To compare and measure variability of the moment and angle profiles, we performed a paired *t*-test between all 100 points of the profiles of CTRL and MASS, MASS and 0%, 0% and 33%, 0% and 66%, and 0% and 100% conditions, which was also verified by a false discovery rate control, as explained in [58]. The periods where the two profiles are statistically different are identified by horizontal brackets in Fig. 6. The angle and moment profiles of the conditions (similar pairs of conditions used for the *t*-test) were compared using a linear regression between the intersubject mean profiles in these two conditions, as explained in [3]. The coefficient of determination (R^2) value of the regression indicates the degree of similarity of the patterns, while the slope refers to the scaling factor. For example, a profile identical to the baseline profile would have an R^2 value and a scale of 1; whereas, a downscaled profile (i.e., smaller range of values) with identical pattern would have $R^2 = 1$ and slope < 1 . One should note that the scale is not very meaningful when R^2 is relatively low.

G. Moment-Angle Analysis

In previous sections, we explained the method to calculate the knee complex's joint angles and moments for conditions 3–6, which included the exoskeletons. Fig. 7 include the intersubject mean moment-angle plots across all the conditions with linear fits to the weight acceptance phase. To obtain the quasi-stiffness of the knee complex (K_C) and of the anatomical knee joint (K_K), linear polynomials were, respectively, regressed on

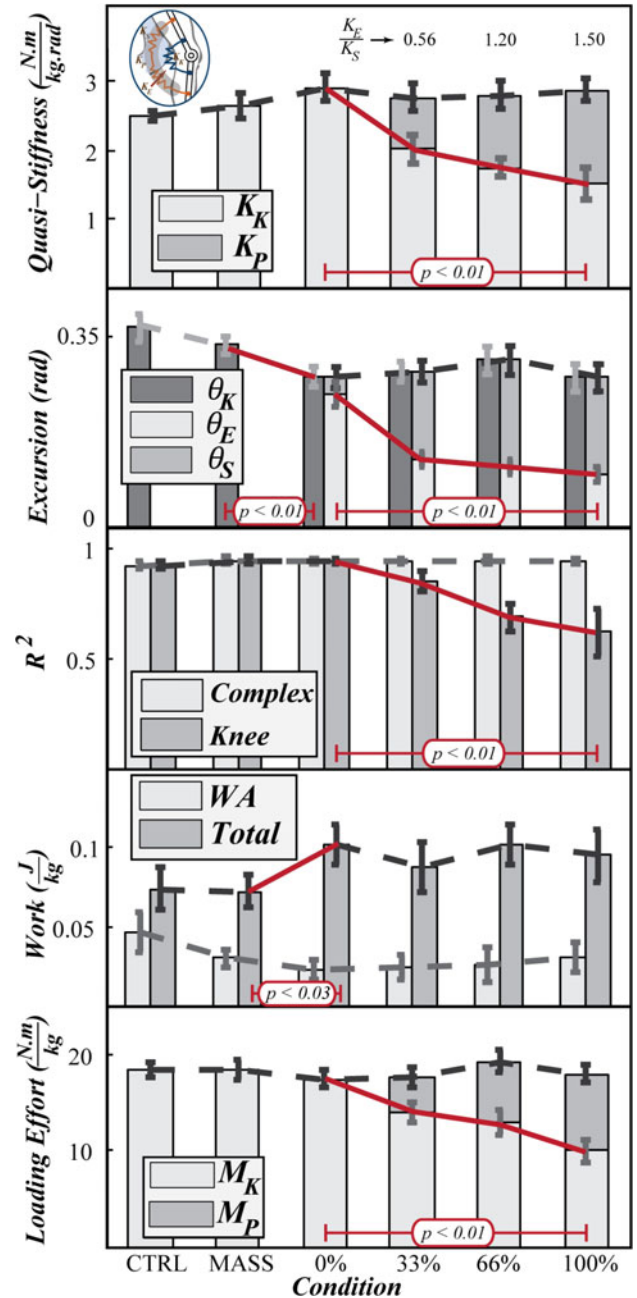


Fig. 8. Intersubject moment-angle analysis of the knee complex, joint, and exoskeleton in the sagittal plane. The first to fifth rows are, respectively, the intersubject mean and ± 1 SD of knee complex quasi-stiffness, excursion, R^2 , work, and loading efforts during the weight acceptance phase. The knee complex joint is a virtual joint composed of the knee joint and exoskeleton joint. The subscript *C* stands for the knee complex, *K* for the knee joint, and *P* for the parallel component, which comprises the exoskeleton and soft tissues. The subscript *S* stands for the series soft tissues and *E* for the exoskeleton. Note that M_K and M_P are calculated as the integral of the moment profiles of the knee joint and exoskeleton. Red lines indicate a statistically significant ($p < 0.05$) difference between adjacent conditions in the graphs, whereas dashed lines indicate no statistically significant change.

the moment-angle data of the knee complex and knee joint in the weight acceptance phase of the gait cycle (as illustrated in Fig. 2). The slopes of the corresponding linear fits represent K_C and K_K , and the R^2 indicates the goodness of the fit representative of the linearity of the behavior of the knee complex and knee

joint in the weight acceptance phase. K_K was subtracted from K_C to calculate K_P and (7) was used to calculate K_S . We also define θ_C as the excursion of the knee complex, θ_K the excursion of the knee joint, θ_E the excursion of the exoskeleton, and θ_S is the excursion of the interface. We subtracted the minimum angle from maximum angle of the knee complex in the weight acceptance phase to calculate θ_C or θ_K (Note that $\theta_C = \theta_K$). We similarly calculated θ_E by subtracting the minimum from maximum angles of the exoskeleton in the weight acceptance phase, and θ_S by subtracting θ_E from θ_C .

This study also aimed to investigate whether an external parallel spring can help to reduce the human knee joint moment in the weight acceptance phase of gait and to what extent. To address this question, the loading effort of the knee joint (M_K) and complex (M_C) were, respectively, defined as the integral of the moment profiles of the knee joint and knee complex in the weight acceptance phase. Parallel assistance (M_P) was defined as the integral of the parallel/exoskeletal moment profile in the weight acceptance phase of gait. These parameters allowed us to investigate the overall effect of the exoskeleton assistance on the reduction of the knee moment throughout the weight acceptance phase of gait. Finally, the mechanical work of the knee joint in the weight acceptance phase and the entire gait cycle were calculated as the area enclosed in the moment-angle graphs of the corresponding period. The aforementioned parameters are plotted in Fig. 8. One should note that the knee complex and knee joint were identical for CTRL and MASS conditions, due to the lack of external exoskeleton joints or parallel stiffness in those conditions.

To study the effect of exoskeleton mass and articulation, a pairwise comparison was performed between the values of quasi-stiffness (K_C and K_K), excursion, R^2 , work, and loading efforts of CTRL and MASS, and MASS and 0% conditions using t -test with a significance level of 0.05. To study the effect of the externally applied parallel stiffness, a one-way ANOVA was performed on the aforementioned parameters for conditions 0%, 33%, 66%, and 100% in addition to a post hoc t -test with Bonferroni correction leading to a significance level of 0.008. In Fig. 8, we have connected the values by thin dashed lines if no statistically significant difference was found (i.e., invariant behavior) and by red lines when the p -value indicated otherwise (i.e., significant behavior change).

H. Knee Response to Parallel Stiffness

We investigated the locomotor response of the knee joint to externally applied parallel stiffnesses in terms of variations of: 1) the quasi-stiffness of the knee joint and complex as functions of the parallel stiffness, and 2) the loading efforts of the knee joint and complex as functions of the parallel assistance. These analyses included the gait cycle for the left and right legs across only the assistance trials (namely conditions 3–6, which correspond to 0% to 100% of the knee quasi-stiffness, respectively).

The values of quasi-stiffnesses and loading efforts were normalized with respect to the intrasubject mean values for the 0% condition. The normalized quasi-stiffnesses of the knee joint (κ_K) was obtained from K_K values in conditions 3–6 (0%, 33%, 66%, and 100%) divided by the intrasubject mean of K_K

in the 0% condition for the corresponding subject, which is assumed as the baseline for that subject. The normalized quasi-stiffnesses of the knee complex (κ_C) were calculated in a similar manner for each subject. It is worth noting that that $K_K = K_C$ in the 0% condition. The normalized parallel stiffness (κ_P) was also obtained by dividing K_P by the intrasubject mean value of K_K in the 0% condition for each subject.

In a similar fashion, the normalized loading effort of the knee joint (M_K) and complex (M_C) were obtained by, respectively, dividing M_K and M_C by their intrasubject mean values in the 0% condition, and the normalized parallel assistance (M_P) by dividing M_P for each gait cycle by the intrasubject mean values of M_K in the 0% condition for each subject.

Finally, the normalized knee joint and complex quasi-stiffnesses (κ_K and κ_C , respectively) were plotted with respect to the normalized external parallel stiffness (κ_P), and the normalized loading efforts of the knee joint and complex (M_K and M_C , respectively) with respect to the normalized exoskeleton assistance (M_P) as shown in Fig. 9. The theoretical (3) and (4) as well as the linear fits were also plotted on the corresponding graphs to compare with the experimental values (see Fig. 9).

III. RESULTS

A. Kinematic and Kinetic Profiles

Fig. 6 includes the angle profiles on the top half and moment profiles on the bottom half for the lower extremity joints in the sagittal plane.

1) *Effect of Mass*: The values of $R^2 = 100\%$ and scale = 0.99 to 1.07 for the angle profiles in Fig. 6 (graphs 1–3) show that the exoskeleton mass did not notably change the overall kinematic patterns of gait in the sagittal plane. However, the exoskeleton mass resulted in a significantly more extended knee in the terminal stance phase and more flexed knee at the heel contact with the ground (note the dark gray stripes on graph 2), which is in agreement with previous results [44]. The values of $R^2 = 99\%$ to 100% and scale = 1.05 to 1.11 for the moment profiles in Fig. 6 (graphs 4–6) show that the exoskeleton mass did not notably change the moment profiles patterns in the sagittal plane but led to a slight overall upscale in the moment profiles.

2) *Effect of Exoskeleton Articulation*: The values of $R^2 = 99\%$ and scale = 0.98 to 1.00 for the angle profiles in Fig. 6 (graphs 7–9) show that the kinematic constraint imposed by the exoskeleton articulation did not notably affect the knee angle patterns and profiles in the sagittal plane. However, the knee joint was significantly more extended during the heel contact and terminal stance phase (note the horizontal brackets on graph 8). The values of $R^2 = 98\%$ to 99% and scale = 0.93 to 1 for the moment profiles of the hip and ankle joints in Fig. 6 (graphs 10–12) show that the exoskeleton articulation does not notably affect the moment patterns of the hip and ankle but led to an overall downscale in the knee moment profile. Particularly, the moment profile of the knee complex did not show a pattern change ($R^2 = 98\%$), but showed a notable downscale (scale = 0.93) under the effect of the exoskeleton articulation.

3) *Effect of Exoskeletal Stiffness*: The values of $R^2 = 99\%$ to 100% for the ankle and hip angle and moment profiles for conditions 33%, 66%, and 100% in Fig. 6 (graphs 13–30) show

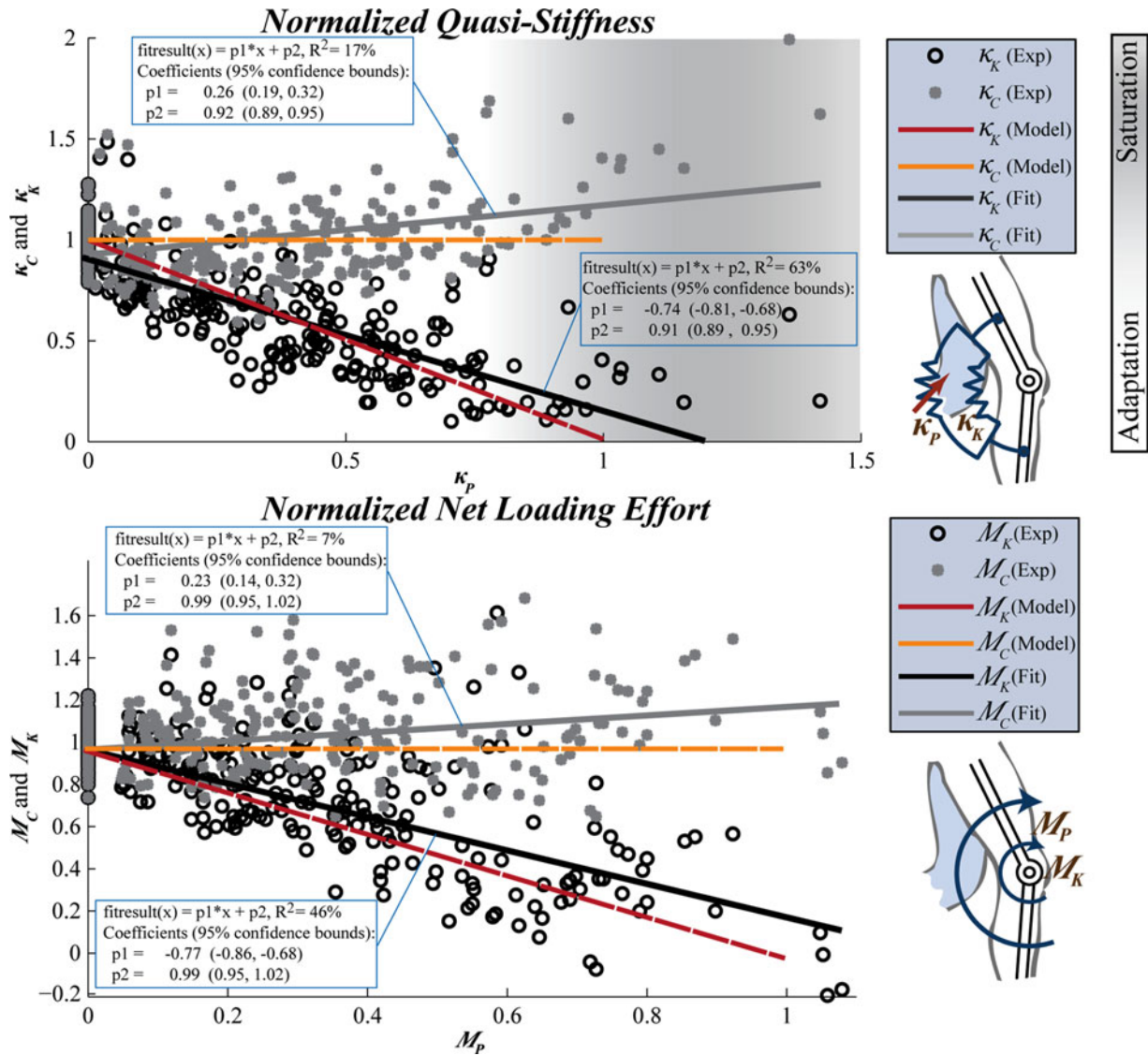


Fig. 9. Top: Normalized quasi-stiffness of the knee complex and joint with respect to the normalized parallel stiffness. Following a trend predicted by the hypothesized equation for the knee stiffnesses ($K_C = K_K + K_P$), the knee joint quasi-stiffness decreases as the parallel stiffness increases up to ~80% of the knee quasi-stiffnesses. For parallel stiffnesses of more than ~80%, the knee joint quasi-stiffness does not follow the hypothesized equation and remains relatively constant leading to an increase in the knee complex quasi-stiffness. Bottom: Normalized loading effort of the knee complex and joint with respect to normalized parallel assistance. The knee joint moment reduces as the parallel assistive moment increases, as predicted by the hypothesized equation for the joint moments ($M_C = M_K + M_P$).

that the external assistance did not have a considerable effect on the overall kinematic and kinetic patterns for those joints in the sagittal plane. It is worth mentioning that the hip angle profile started to deviate from the baseline at high exoskeletal stiffness (note the horizontal brackets on graph 27). The angle and moment profiles of the knee complex exhibited invariant overall patterns under the exoskeleton assistance ($R^2 = 98\%$ to 99%), with significant local variations in the angle profiles at the initial stance and terminal swing phase (notice the horizontal brackets on graphs 14, 20, and 26) and significant local variation in the moment profile at the initial swing phase (note the horizontal brackets on graphs 17, 23, and 29). A slight downscale in the values of the angle profiles of the knee and hip in the sagittal plane was observed, and an upscale in the values of the knee and hip moments was observed in the sagittal plane.

B. Moment-Angle Performance of the Knee Complex

Fig. 8 shows the parameters that explain intersubject moment-angle behavior of the knee in the weight acceptance phase of gait. The first to third rows, respectively, include the quasi-stiffness (K_C and K_K), excursion, and R^2 of the weight acceptance phase, the fourth row includes the mechanical work of the weight acceptance phase and entire gait cycle, and the fifth row includes the loading efforts of the weight acceptance phase. The dashed lines illustrate the trends, while the solid lines in red and the p -values indicate those values that are statistically different from the baseline measure, according to the statistical comparison explained in Section-II.

1) *Quasi-Stiffness*: The intersubject mean and SD of the knee complex quasi-stiffness in the weight acceptance phase

are shown in the first row of Fig. 8. The values of the knee joint quasi-stiffness (K_K) and parallel stiffness (K_P) are also reported using different colors in the bar graph [see Fig. 8 (top row)]. A nonsignificant increase in K_C was observed as a result of the exoskeleton mass and as a result of the exoskeleton articulations. K_C remained invariant across the assistance conditions (33%–100%). However, a significant ($p < 0.008$) decrease in the knee joint quasi-stiffness (K_K) relative to the 0% condition was observed for each level of exoskeletal assistance (33%, 66%, and 100%).

Columns 7 and 8 of Table III report the measured and estimated quasi-stiffnesses across the subjects, respectively. Comparing these two columns give us the average error of estimation of our models as $\sim 33\%$. The first row of Fig. 8 also includes the ratio of K_E/K_S , which in combination with the value of K_P and using (7), we can estimate K_S . We skipped this analysis because we calculated it in our previous work and it was outside the scope of this paper [56].

2) *Excursion*: The intersubject mean and SD of the knee joint excursion (θ_K), exoskeleton excursion (θ_E), and soft-tissue excursion (θ_S) in the weight acceptance phase are shown in the second row of Fig. 8. A nonsignificant decrease in θ_K was observed in MASS condition relative to CTRL condition and a significant decrease for the knee excursion in 0% condition relative to MASS condition ($p < 0.05$). The knee excursion remained relatively constant across the different assistance conditions. However, θ_E significantly decreased with exoskeleton assistance (33%, 66%, and 100%) as compared to the 0% condition ($p < 0.008$).

3) *Linearity of the Knee Behavior*: The intersubject mean and SD of the R^2 values for the linear fits to the moment-angle graphs of the knee complex and knee joint in the weight acceptance phase are shown in the third row of Fig. 8. There was no significant change in R^2 values for the knee complex across all of the conditions implying that the overall behavior of the knee complex remained linear. However, a significant reduction ($p < 0.008$) in R^2 values was observed for the knee joint across the assistance conditions (33%, 66%, and 100%) relative to the 0% condition.

4) *Mechanical Work*: The intersubject mean and SD of the knee joint mechanical work in the weight acceptance (WA) phase and throughout the entire gait cycle (Total) are shown in the fourth row of Fig. 8. No significant changes in the mechanical work of the knee joint in the weight acceptance phase and throughout the gait cycle were observed; except a significant increase ($p < 0.05$) in the entire gait cycle work was observed for the 0% condition as compared to the MASS condition.

5) *Loading Effort*: The intersubject mean and SD of the loading efforts (integral of the moment profile) of the knee joint and complex as well as the exoskeleton assistance are shown in the fifth row of Fig. 8. A significant ($p < 0.008$) decrease in the loading effort of the knee joint was observed with the exoskeletal assistance conditions (conditions 4–6) as compared to the 0% condition (condition 3). The values of M_C (equal to $M_K + M_P$) do not exhibit a significant change across the conditions.

C. Changes in Knee Moment and Quasi-Stiffness

Fig. 9 (top) shows the graph of the normalized quasi-stiffness of the knee joint and complex (κ_K and κ_C , respectively) against the normalized parallel stiffness (κ_P). Fig. 9 (bottom) shows the graph of normalized loading effort of the knee joint and complex (\mathcal{M}_K and \mathcal{M}_C , respectively) against the normalized parallel assistance (\mathcal{M}_P).

As seen in Fig. 9, the theoretical models are in close agreement with the trends of the experimental values of κ_K and κ_C . Starting at around $\kappa_P \approx 0.8$, however, the experimental values start to deviate from the theoretical models. In particular, κ_K tends to remain relatively constant and κ_C tends to increase. The cutoff value of $\kappa_P \approx 0.8$ was determined by *visual inspection* and not from the data, because the values of κ_P do not span a wide enough range to apply statistical methods to quantitatively find the cutoff quasi-stiffness. In contrast, the experimental values of \mathcal{M}_K and \mathcal{M}_C appear to follow the theoretical models throughout the range of experimental values of \mathcal{M}_P .

The theoretical models explained by (3) and (4) are also plotted on each graph (dashed lines) of Fig. 9. Linear polynomials were regressed to the quasi-stiffness and loading effort data with the 95% confidence intervals, as shown in Fig. 9. According to these fits, there is a slight but significant difference between the model [described by (3) and (4)] and the experimental values of the quasi-stiffness and loading effort, with (4) matching more closely the experimental loading effort data. Fig. 9 only includes the gait cycle data for the exoskeletal assistance conditions (0% to 100%).

IV. DISCUSSION

In this paper, we experimentally studied the motor response and biomechanical changes in lower extremity joints to external stiffness applied in parallel with the knee joint. The external stiffness was applied only during the weight acceptance phase of gait, in which the knee behaves close to a linear torsional spring. The experimental results revealed that the lower extremity joints undergo substantial motor changes in response to parallel stiffness, while the kinematic and kinetic patterns remain invariant. The exoskeleton mass did not impose notable disturbance on the moment and angle patterns but resulted in an overall higher range of joint moments. The exoskeleton articulation was found to impose negligible kinematic and kinetic constraints on the overall angle and moment patterns implying that a simple uniaxial hinge joint can be a viable design choice for knee exoskeletons. The exoskeleton mass, articulation, and stiffness were mostly found to locally affect the knee joint moment and angle profiles around the initial and terminal stance as well as the terminal swing phase.

A detailed analysis of the moment angle of the knee joint in the weight acceptance phase revealed that the knee joint quasi-stiffness changes in response to an externally applied stiffness such that the overall quasi-stiffness of the complex of the knee joint and exoskeleton remains invariant; the same behavior was observed for the knee joint and knee complex moments. However, the exoskeleton mass and articulation does not affect the knee joint quasi-stiffness and loading effort. Moreover, the exoskeleton assistance affected the linearity of the moment-angle

TABLE III
DEMOGRAPHIC DATA OF THE PARTICIPANTS AS WELL AS THE STIFFNESS OF THE EXOSKELETON SPRINGS AND TIMING OF DISENGAGEMENT

No.	Gender	Age	Height (m)	Mass (kg)	Preferred Gait Speed (m/s)	Measured Quasi-Stiffness (Nm/rad)	Estimated Quasi-Stiffness (Nm/rad)	33% Exoskeleton Stiffness (Nm/rad)	Disengagement Time (%Stride)	66% Exoskeleton Stiffness (Nm/rad)	Disengagement Time (%Stride)	100% Exoskeleton Stiffness (Nm/rad)	Disengagement Time (%Stride)
1	F	24	1.70	79.9	1.43	258	274	92	40	174	35	239	36
2	M	24	1.69	78.5	1.39	257	267	89	41	174	30	239	31
3	M	26	1.83	68.0	1.21	117	247	81	26	160	29	239	29
4	M	23	1.68	71.0	1.12	156	240	81	29	160	29	239	31
5	M	29	1.77	66.7	1.21	149	235	81	36	160	37	239	36
6	M	18	1.80	68.0	1.43	143	243	82	34	166	28	239	36
7	M	22	1.76	67.0	1.03	110	235	81	21	160	21	239	20
8	M	21	1.89	103.8	1.34	318	393	128	35	239	36	328	32
9	M	22	1.73	86.0	1.30	321	299	103	27	203	31	328	30
	Mean	23.2	1.76	76.5	1.27	203	270	91	32	177	30	259	31
	SD	3.1	0.1	12.3	0.14	85	51	16	6	27	4	39	5

behavior of the knee joint as suggested by the significant reduction of the R^2 values of the linear fits to the moment-angle data of the knee joint in the weight acceptance phase decreased as the exoskeleton assistance increased. On the contrary, the overall moment-angle behavior of the knee complex remained linear with R^2 values abiding near 1 in all experimental conditions. This finding suggests that humans regulate their lower limb biomechanics so that they experience an overall linear behavior at the knee joint during the weight acceptance phase, which could be associated with higher rates of energy recovery [22], [44]. The exoskeleton stiffness did not have a significant effect on the mechanical work of the knee joint in the weight acceptance phase implying that the assistance provided by the exoskeletal stiffness did not require additional mechanical work.

The analysis of the knee joint quasi-stiffness response to parallel stiffness showed that the knee joint exhibits smaller quasi-stiffness in the presence of a parallel stiffness such that the overall quasi-stiffness remains invariant. The knee joint quasi-stiffness progressively changed in response to increasing parallel stiffness, but saturated when the parallel stiffness reached *approximately* ~80% of natural knee quasi-stiffness. After this approximate value, the knee joint quasi-stiffness remained relatively constant, and any further increase in the parallel stiffness caused an increase in the overall knee complex quasi-stiffness. Furthermore, it was observed that the loading effort of the knee joint showed a significant reduction in response to parallel assistance suggesting that the knee joint can fully accommodate for the external assistance. We should point out that the exact value of the saturation quasi-stiffness was not quantitatively obtained due to the limited range of parallel stiffnesses tested.

The saturation of the quasi-stiffness behavior could be attributable to the existence of biarticular muscles leading us to speculate that the exoskeletal assistance can only unload the monoarticular muscles to avoid any alteration in the behavior of neighboring joints spanned by the biarticular. Future research is needed to investigate this hypothesis through analysis of the EMG signals of monoarticular and biarticular muscles.

The findings from this experimental work can give an insight to the design of exoskeletons/orthoses for lower extremity joints (specifically the knee joint). Replication of the moment-angle behavior of the lower extremity joints by an exoskeletal

device can be a viable strategy to assist and unload this joint. The compliance of the biological soft tissues of the leg as well as the interface components of the exoskeleton can neutralize the assistance of the exoskeletons. This is especially true for exoskeletons attached to the thighs, due to the large amount of soft tissue located at those segments. Therefore, the design of exoskeletons should minimize the effect of the soft tissues with additional considerations such as larger pads and more carefully chosen strap locations. Moreover, the control algorithm of the exoskeletons should not solely rely on the angular movement of the exoskeleton that could be disturbed by the excursion of the soft tissues.

The exoskeleton uniaxial joint did not substantially perturb the gait patterns implying that a uniaxial joint can be a suitable choice in the design of knee exoskeletons. The kinematic constraints imposed by the exoskeleton joint resulted in a slightly more flexed knee at the heel strike, which could be a result of limited range of motion of the exoskeleton joints (as fabrication imperfection), as it was reported by the participants about the left exoskeleton. In another study, we found that the exoskeleton mass is the main contributor to the increase in the metabolic cost of walking [59]. Here, we found that the exoskeleton mass caused an upscale in the range of joint moments suggesting that minimization of the exoskeleton mass should be a main goal in the design of exoskeletons. The knee joint complex behaved linearly under all six conditions implying that the human body prefers to experience a linear behavior at the knee complex. This preferred linear behavior may be related to the energetics of gait, the damping function of the knee, or the preferred gait speed [44], [60]–[62]. Regardless of the reason, a knee exoskeleton ideally should demonstrate a linear behavior in the weight acceptance phase of gait as shown here.

This study necessitated several assumptions. The reflective markers of this study were mounted on the skin of the volunteer; hence, the kinematic profiles of the knee complex and anatomical joint are assumed to be identical. The exoskeleton was suspended from the shoulders using a pair of suspension harnesses to limit the vertical migration of the exoskeleton. These suspension straps may have caused confounding factors in the results and affected the kinetic and kinematic behavior of the joints.

To carry out the inverse dynamics analysis, several assumptions were made. The knee joint and exoskeleton were considered one single joint. Despite the independence of the inverse dynamics analysis of the morphology of the joints, this assumption can have nuisance effects on the joint center estimations and the calculations of the kinetic profiles. The exoskeleton moment of inertia and center of mass were obtained from a computer-aided design model of the exoskeleton and exoskeleton replica, which ignores the effect of small movements of the exoskeleton with respect to the limbs and slight differences between the actual device and the computer models. Furthermore, it should be noted that as the exoskeletal stiffness increased the knee joint behavior became less linear (lower R^2 values, Fig. 8), which could make the calculations of the knee joint quasi-stiffness less accurate and the linear models of (3) and (4) less accurate.

The knee joint levels of quasi-stiffness in the 33%, 66%, and 100% conditions were estimated using a previously developed statistical model, because *a priori* knowledge of the natural knee quasi-stiffness of each volunteer was not available [22], [39]. The estimation models were developed in previous studies for design of lower extremity orthoses and prostheses [20]–[22]. Table III lists the knee quasi-stiffness of each volunteer for the CTRL condition as calculated using the moment-angle data, which shows that the values estimated using the models are different from the experimental values. This inaccuracy was addressed by normalizing the quasi-stiffness of each assistance level (0%, 33%, 66%, and 100%) by the natural knee stiffness measured during the 0% condition for each volunteer in the analysis of motor response presented in Fig. 9. One can see that some data points have normalized parallel stiffness of $\sim 150\%$, which is the result of the error in the initial estimation of the knee quasi-stiffness.

Another limitation of this study is the method of estimation of the exoskeleton moment. Currently, we calculate the exoskeleton moment by multiplying the stiffness of the exoskeleton by the flexion of the exoskeleton using (6), rather than through instrumentation of the device. We chose not to include load cell in the exoskeleton to minimize the exoskeleton mass, and to minimize the number of wires attached to the subjects during the experiment. Ideally, we would have incorporated a force measuring device to directly measure the moment of the exoskeleton. In previous studies, we characterized the moment-angle behavior of the exoskeletons [56], [63].

To study the changes in the knee joint moment, we examined the correlation between the loading effort, which is the summation of the knee joint moments and knee complex moments during the weight acceptance phase and parallel assistance, which is the summation of the exoskeleton moments during the weight acceptance phase. Alternatively, we could have investigated the maximum moment of the knee joint and complex in the weight acceptance phase. However, for some of the trials, we observed that the exoskeleton springs disengaged before the end of the weight acceptance phase (as detailed in Table III) depending on the gait patterns and timing of the toe and heel contact with the ground. Therefore, using the maximum moment of the knee joint and complex would not have given a complete picture of the effect of the exoskeleton assistance on the knee joint loading effort throughout the weight acceptance phase.

As future steps for this research, we intend to investigate the EMG activities of the muscles adjacent to the knee joint and analyze the performance of both monoarticular and biarticular muscles in interaction with the exoskeleton. We also intend to analyze the behavior of the adjacent joints (i.e., ankle and hip) under the effect of assistance to the knee joint to examine the locality of the external stiffness effects. Finally, we intend to investigate the effect of the exoskeleton on the metabolic cost of locomotion [59].

V. CONCLUSION

In this study, we found that a spring in parallel with the knee joint can help to unload the knee joint during the stance phase. We also found that the knee joint can accommodate a parallel spring with a wide range of stiffness up to $\sim 80\%$ of the natural knee quasi-stiffness, after which the parallel spring still provides assistance but the knee complex stiffness increases above the normal rate. This finding also supports the assumption that the knee joint can be theoretically modeled by a linear torsional spring in the weight acceptance phase of gait. We also found that a uniaxial joint is a viable design choice for a knee exoskeleton. The exoskeleton mass was found to be the major contributor to the increase in the joint moments implying that future design efforts should focus on mass minimization.

REFERENCES

- [1] D. Ferris *et al.*, "Neuromechanical adaptation to hopping with an elastic ankle-foot orthosis," *J. Appl. Physiol.*, vol. 100, no. 1, pp. 163–170, 2006.
- [2] G. Sawicki *et al.*, "The effects of powered ankle-foot orthoses on joint kinematics and muscle activation during walking in individuals with incomplete spinal cord injury," *J. Neuroeng. Rehabil.*, vol. 3, pp. 1–17, 2006.
- [3] P. Kao *et al.*, "Invariant ankle moment patterns when walking with and without a robotic ankle exoskeleton," *J. Biomech.*, vol. 43, no. 2, pp. 203–209, 2010.
- [4] P. Kao *et al.*, "Short-term locomotor adaptation to a robotic ankle exoskeleton does not alter soleus Hoffmann reflex amplitude," *J. Neuroeng. Rehabil.*, vol. 7, no. 33, pp. 1–8, 2010.
- [5] A. Dollar and H. Herr, "Lower extremity exoskeletons and active orthoses: Challenges and state-of-the-art," *IEEE Trans. Robot.*, vol. 24, no. 1, pp. 144–158, Feb. 2008.
- [6] M. Eilenberg *et al.*, "Control of a powered ankle-foot prosthesis based on a neuromuscular model," *IEEE Trans. Neural Syst. Rehabil. Eng.*, vol. 18, no. 2, pp. 164–173, Apr. 2010.
- [7] S. Jezernik *et al.*, "Automatic gait-pattern adaptation algorithms for rehabilitation with a 4-DOF robotic orthosis," *IEEE Trans. Robot. Autom.*, vol. 20, no. 3, pp. 574–582, Jun. 2004.
- [8] L. Marchal-Crespo and D. Reinkensmeyer, "Review of control strategies for robotic movement training after neurologic injury," *J. Neuroeng. Rehabil.*, vol. 6, pp. 1–15, 2009.
- [9] D. Ferris *et al.*, "Powered lower limb orthoses for gait rehabilitation," *Topics Spinal Cord Injury Rehabil.*, vol. 11, no. 2, pp. 34–49, 2005.
- [10] D. Ferris and C. Farley, "Interaction of leg stiffness and surface stiffness during human hopping," *J. Appl. Physiol.*, vol. 82, no. 1, pp. 15–22, 1997.
- [11] J. Ortega and C. Farley, "Minimizing center of mass vertical movement increases metabolic cost in walking," *J. Appl. Physiol.*, vol. 99, no. 6, pp. 2099–2107, 2005.
- [12] J. Choi and A. Bastian, "Adaptation reveals independent control networks for human walking," *Nature Neurosci.*, vol. 10, no. 8, pp. 1055–1062, 2007.
- [13] A. Roy *et al.*, "Measurement of human ankle stiffness using the anklebot," in *Proc. IEEE 10th Int. Conf. Rehabil. Robot.*, 2007, pp. 356–363.
- [14] R. Browning *et al.*, "The effects of adding mass to the legs on the energetics and biomechanics of walking," *Med. Sci. Sports Exercise*, vol. 39, no. 3, pp. 515–525, 2007.

- [15] T. Royer and P. Martin, "Manipulations of leg mass and moment of inertia: Effects on energy cost of walking," *Med. Sci. Sports Exercise*, vol. 37, no. 4, pp. 649–656, 2005.
- [16] A. Birn-Jeffery and M. Daley, "Birds achieve high robustness in uneven terrain through active control of landing conditions," *J. Exp. Biol.*, vol. 215, no. 12, pp. 2117–2127, 2012.
- [17] H. van Hedel *et al.*, "Obstacle avoidance during human walking: Transfer of motor skill from one leg to the other," *J. Physiol.-Lond.*, vol. 543, no. 2, pp. 709–717, 2002.
- [18] H. Geyer *et al.*, "Compliant leg behaviour explains basic dynamics of walking and running," in *Proc. Roy. Soc. B-Biol. Sci.*, vol. 273, no. 1603, pp. 2861–2867, 2006.
- [19] M. Gunther and R. Blickhan, "Joint stiffness of the ankle and the knee in running," *J. Biomech.*, vol. 35, no. 11, pp. 1459–1474, 2002.
- [20] K. Shamaei *et al.*, "Estimation of quasi-stiffness and propulsive work of the human ankle in the stance phase of walking," *PLoS ONE*, vol. 8, no. 3, p. e59935, 2013.
- [21] K. Shamaei *et al.*, "Estimation of quasi-stiffness of the human hip in the stance phase of walking," *PLoS ONE*, vol. 8, no. 12, p. e81841, 2013.
- [22] K. Shamaei *et al.*, "Estimation of quasi-stiffness of the human knee in the stance phase of walking," *PLoS ONE*, vol. 8, no. 3, p. e59993, 2013.
- [23] P. Weiss *et al.*, "Position dependence of ankle joint dynamics: I. Passive mechanics," *J. Biomech.*, vol. 19, no. 9, pp. 727–735, 1986.
- [24] R. Kearney *et al.*, "Identification of intrinsic and reflex contributions to human ankle stiffness dynamics," *IEEE Trans. Biomed. Eng.*, vol. 44, no. 6, pp. 493–504, Jun. 1997.
- [25] G. Smidt, "Biomechanical analysis of knee flexion and extension," *J. Biomech.*, vol. 6, no. 1, pp. 79–92, 1973.
- [26] A. Biewener and G. Gillis, "Dynamics of muscle function during locomotion: Accommodating variable conditions," *J. Exp. Biol.*, vol. 202, no. 23, pp. 3387–3396, 1999.
- [27] J. Dean and A. Kuo, "Energetic costs of producing muscle work and force in a cyclical human bouncing task," *J. Appl. Physiol.*, vol. 110, no. 4, pp. 873–880, 2011.
- [28] W. Farahat and H. Herr, "Optimal workloop energetics of muscle-actuated systems: An impedance matching view," *Plos Comput. Biol.*, vol. 6, no. 6, p. e1000795, 2010.
- [29] C. Farley *et al.*, "Mechanism of leg stiffness adjustment for hopping on surfaces of different stiffnesses," *J. Appl. Physiol.*, vol. 85, no. 3, pp. 1044–1055, 1998.
- [30] A. Kerdok *et al.*, "Energetics and mechanics of human running on surfaces of different stiffnesses," *J. Appl. Physiol.*, vol. 92, no. 2, pp. 469–478, 2002.
- [31] G. Elliott *et al.*, "The biomechanics and energetics of human running using an elastic knee exoskeleton," presented at the IEEE Conf. Rehabil. Robot., Seattle, WA, USA, 2013.
- [32] M. Cherry *et al.*, "Design and fabrication of an elastic knee orthosis: Preliminary results," presented at the (ASME Int. Des. Eng. Tech. Conf. Comput. Inf. Eng. Conf., Philadelphia, PA, USA, 2006.
- [33] A. Grabowski and H. Herr, "Leg exoskeleton reduces the metabolic cost of human hopping," *J. Appl. Physiol.*, vol. 107, no. 3, pp. 670–678, 2009.
- [34] D. Farris and G. Sawicki, "Linking the mechanics and energetics of hopping with elastic ankle exoskeletons," *J. Appl. Physiol.*, vol. 113, no. 12, pp. 1862–1872, 2012.
- [35] T. Lenzi *et al.*, "Powered hip exoskeletons can reduce the user's hip and ankle muscle activations during walking," *IEEE Trans. Neural Syst. Rehabil. Eng.*, vol. 21, no. 6, pp. 938–948, Nov. 2013.
- [36] K. Gregorczyk *et al.*, "Effects of a lower-body exoskeleton device on metabolic cost and gait biomechanics during load carriage," *Ergonomics*, vol. 53, no. 10, pp. 1263–1275, 2010.
- [37] G. Colombo *et al.*, "Treadmill training of paraplegic patients using a robotic orthosis," *J. Rehabil. Res. Dev.*, vol. 37, no. 6, pp. 693–700, 2000.
- [38] J. Veneman *et al.*, "Design and evaluation of the LOPES exoskeleton robot for interactive gait rehabilitation," *IEEE Trans. Neural Syst. Rehabil. Eng.*, vol. 15, no. 3, pp. 379–386, Sep. 2007.
- [39] K. Shamaei *et al.*, "A quasi-passive compliant stance control knee-ankle-foot orthosis," presented at the IEEE Int. Conf. Rehabil. Robot., Seattle, WA, USA, 2013.
- [40] S. Irby *et al.*, "Gait of stance control orthosis users: The dynamic knee brace system," *Prosthetics Orthotics Int.*, vol. 29, no. 3, pp. 269–282, 2005.
- [41] B. Zacharias and A. Kannenberg, "Clinical benefits of stance control orthosis systems: An analysis of the scientific literature," *J. Prosthetics Orthotics*, vol. 24, no. 1, pp. 2–7, 2012.
- [42] A. Blanchette *et al.*, "Walking while resisting a perturbation: Effects on ankle dorsiflexor activation during swing and potential for rehabilitation," *Gait Posture*, vol. 34, no. 3, pp. 358–363, 2011.
- [43] C. Walsh *et al.*, "A quasi-passive leg exoskeleton for load-carrying augmentation," *Int. J. Humanoid Robot.*, vol. 4, no. 3, pp. 487–506, 2007.
- [44] K. Shamaei and A. Dollar, "On the mechanics of the knee during the stance phase of the gait," presented at the IEEE Int. Conf. Rehabil. Robot., Zurich, Switzerland, 2011.
- [45] J. Perry, *Gait Analysis: Normal and Pathological Function*. Thorofare, NJ, USA: SLACK, 1992.
- [46] J. Rose and J. Gamble, *Human Walking*. Philadelphia, PA, USA: Williams & Wilkins, 2006.
- [47] D. Winter, *The Biomechanics and Motor Control of Human Gait: Normal, Elderly and Pathological*, 2nd ed. Waterloo, ON, Canada: Univ. Waterloo Press, 1991.
- [48] S. Mochon and T. McMahon, "Ballistic walking—An improved model," *Math. Biosci.*, vol. 52, no. 3, pp. 241–260, 1980.
- [49] R. Davis, and P. DeLuca, "Gait characterization via dynamic joint stiffness," *Gait Posture*, vol. 4, no. 3, pp. 224–231, 1996.
- [50] D. Stefanyshyn and B. Nigg, "Dynamic angular stiffness of the ankle joint during running and sprinting," *J. Appl. Biomech.*, vol. 14, no. 3, pp. 292–299, 1998.
- [51] P. Crenna and C. Frigo, "Dynamics of the ankle joint analyzed through moment-angle loops during human walking: gender and age effects," *Human Movement Sci.*, vol. 30, no. 6, pp. 1185–1198, 2011.
- [52] C. Frigo *et al.*, "Moment-angle relationship at lower limb joints during human walking at different velocities," *J. Electromyogr. Kinesiol.*, vol. 6, no. 3, pp. 177–190, 1996.
- [53] S. Lark *et al.*, "Joint torques and dynamic joint stiffness in elderly and young men during stepping down," *Clin. Biomech.*, vol. 18, no. 9, pp. 848–855, 2003.
- [54] K. Shamaei *et al.*, "On the mechanics of the ankle in the stance phase of the gait," in *Proc. IEEE Ann. Int. Conf. Eng. Med. Biol. Soc.*, Boston, MA, USA, 2011, pp. 8135–8140.
- [55] I. McClay and K. Manal, "Three-dimensional kinetic analysis of running: significance of secondary planes of motion," *Med. Sci. Sports Exercise*, vol. 31, no. 11, pp. 1629–1637, 1999.
- [56] K. Shamaei *et al.*, "Design and evaluation of a quasi-passive knee exoskeleton for investigation of motor adaptation in lower extremity joints," *IEEE Trans. Biomed. Eng.*, vol. 61, no. 6, pp. 1809–1821, 2014.
- [57] D. Winter, *Biomechanics and Motor Control of Human Movement*, 3rd ed. Hoboken, NJ, USA: Wiley, 2005.
- [58] Y. Benjamini, and Y. Hochberg, "Controlling the false discovery rate: A practical and powerful approach to multiple testing," *J. Roy. Statist. Soc. Ser. B, Methodological*, vol. 57, no. 1, pp. 289–300, 1995.
- [59] K. Shamaei *et al.*, "Preliminary investigation of effects of a quasi-passive knee exoskeleton on gait energetics," in *Proc. IEEE 36th Annu. Int. Conf. Eng. Med. Biol. Soc.*, 2014, pp. 3061–3064.
- [60] S. Gard and D. Childress, "The influence of stance-phase knee flexion on the vertical displacement of the trunk during normal walking," *Arch. Phys. Med. Rehabil.*, vol. 80, no. 1, pp. 26–32, 1999.
- [61] S. Gard and D. Childress, "What determines the vertical displacement of the body during normal walking?" *J. Prosthetics Orthotics*, vol. 13, no. 3, pp. 64–67, 2001.
- [62] A. Minetti, "Invariant aspects of human locomotion in different gravitational environments," *Acta Astronaut.*, vol. 49, nos. 3–10, pp. 191–198, 2001.
- [63] K. Shamaei *et al.*, "Design and functional evaluation of a quasi-passive compliant stance control knee-ankle-foot orthosis," *IEEE Trans. Neural Syst. Rehabil. Eng.*, vol. 22, no. 2, pp. 258–268, May 2014.

Authors' photographs and biographies not available at the time of publication.